BIOCHEMISTRY
including biophysical chemistry & molecular biology

Article

pubs.acs.org/biochemistry

Interaction of Thrombin with Sucrose Octasulfate

Bijoy J. Desai, Rio S. Boothello, Akul Y. Mehta, J. Neel Scarsdale, H. Tonie Wright,* and Umesh R. Desai

Departments of Medicinal Chemistry and Biochemistry and Institute for Structural Biology and Drug Discovery, Virginia Commonwealth University, 800 East Leigh Street, Suite 212, Richmond, Virginia 23219, United States

ABSTRACT: The serine protease thrombin plays multiple roles in many important physiological processes, especially coagulation, where it functions as both a pro- and anticoagulant. The polyanionic glycosaminoglycan heparin modulates thrombin's activity through binding at exosite II. Sucrose octasulfate (SOS) is often used as a surrogate for heparin, but it is not known whether it is an effective heparin mimic in its interaction with thrombin. We have characterized the interaction of SOS with thrombin in solution and determined a crystal structure of their complex. SOS binds thrombin with a K_d of ~1.4 μM, comparable to that of the much larger polymeric heparin measured under the same conditions. Nonionic (hydrogen bonding) interactions make a larger contribution to thrombin binding of SOS than to heparin. SOS binding to exosite II inhibits thrombin's catalytic activity with high potency but with low efficacy. Analytical ultracentrifugation shows that bovine and human thrombins are monomers in solution in the presence of SOS, in contrast to their complexes with heparin, which are dimers. In the X-ray crystal structure, two molecules of SOS are bound nonequivalently to exosite II portions of a thrombin dimer, in contrast to the 1:2 stoichiometry of the heparin–thrombin complex, which has a different monomer association mode in the dimer. SOS and heparin binding to exosite II of thrombin differ on both chemical and structural levels and, perhaps most significantly, in thrombin inhibition. These differences may offer paths to the design of more potent exosite II binding, allosteric small molecules as modulators of thrombin function.

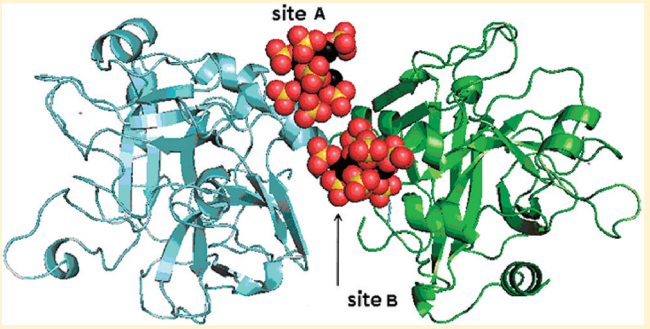

Thrombin plays a major role in the hemostasis/coagulation system[1−4] and is an important mediator of cellular processes, such as activation of platelets,[5,6] monocytes,[7] microglial cells,[8] and dendritic cells,[9] which are implicated in vascular and neural inflammation[8,10,11] and tumor metastasis.[11] Most of these functions are a consequence of thrombin's proteolytic activity. In its hemostatic role, thrombin catalyzes the cleavage of fibrinogen to fibrin monomers, which polymerize with the aid of factor XIIIa to form a clot. Factor XIIIa and several other proteins of the coagulation cascade, e.g., factors Va and VIIIa, are generated through the proteolytic action of thrombin.[11] In direct opposition to this procoagulant role, thrombin also exerts an anticoagulant role by proteolytic processing of protein C in the presence of thrombomodulin, an endothelial cell surface receptor.[11,12] Thrombin's cellular effects arise through its cleavage of protease-activated receptors (PARs), a family of G-protein-coupled receptors present on a large number of cells. Of the four known PARs, thrombin activates isoforms 1, 3, and 4, with major physiological and pathological consequences.[5−8,11,13]

Thrombin's high-specificity interaction with so many substrates is mediated in part by two anion-binding exosites, which are approximately 10−20 Å from its active site. Exosite I is formed by several lysines and arginines interspersed with a few hydrophobic residues and is involved in binding to fibrinogen, fibrin, hirudin, and other proteins.[3,4,14] Diametrically opposed to exosite I is another patch of electropositive residues constituting exosite II, also known as the heparin-binding site. Exosite II consists of Arg93, Arg101, Arg126, Arg165, Arg233, Lys235, Lys236, and Lys240 residues (chymotrypsin numbering) and is an expansive area (~25 Å long) that can accommodate a six-unit fragment of heparin. In addition to interacting with heparin, exosite II engages the anionic chondroitin sulfate moiety present in thrombomodulin[15,16] and also the anionic C-terminal domain of hemeadin, a peptide from the leech *Haemadipsa sylvestri*.[14] A group of chemoenzymatically prepared sulfated low-molecular weight lignins has been found to bind in or near exosite II of thrombin.[17,18]

Exosite I–ligand interactions induce conformational changes in the active site of thrombin, thereby influencing the specificity and reactivity of the protease toward its macromolecular substrates.[4] The ligands also affect the catalytic efficiency (k_{cat}/K_M) of hydrolysis of small peptide substrates, albeit in an unpredictable manner. For example, studies with hirugen, the C-terminal dodecapeptide of hirudin, show that the catalytic efficiency increases or decreases depending on the nature of the chromogenic substrate used to measure activity.[19−24] Likewise, the effect of exosite II ligands on the k_{cat}/K_M of thrombin appears to be ligand-dependent. For example, sulfated lignins

Received: March 26, 2011
Revised: June 23, 2011
Published: July 8, 2011

induce inhibition of proteolytic activity,[17] while heparins do not,[21,22] although the latter affect the fluorescence properties of *p*-aminobenzamidine (PABA) used as an active site probe.[23] An exhaustive re-evaluation of allosteric effects on thrombin function revealed significant ligand-specific coupling between each of the two exosites and the active site, but insignificant interexosite coupling.[24]

Modulation of thrombin's proteolytic activity by exosite ligands affords an opportunity for the development of specific allosteric effectors. It is surprising that despite the plethora of allosteric interactions reported in the literature, nearly all inhibitors of thrombin have been designed to target its active site.[25,26] A primary reason for this is the difficulty of designing small anionic scaffolds that will specifically target the electropositive exosites of thrombin. The exosites are surface-exposed, shallow depressions on the thrombin surface, rather than well-defined, deep binding sites, which typically are easier to target. The high electropositive character of these exosites is likely to attract practically any collection of anions, thereby degrading the specificity of the interaction, as noted with heparin.[23] Finally, the absence of appropriate tools, such as a maneuverable small lead ligand and a molecular modeling protocol, adds to the difficulty of designing allosteric effectors.

With the goal of designing specific, small, synthetic allosteric modulators of thrombin function, we studied the interaction of SOS with BT and HT at the molecular level. SOS is a highly sulfated disaccharide known to mimic polymeric heparin (Figure 1) and to bind in exosite II of thrombin.[27] It may

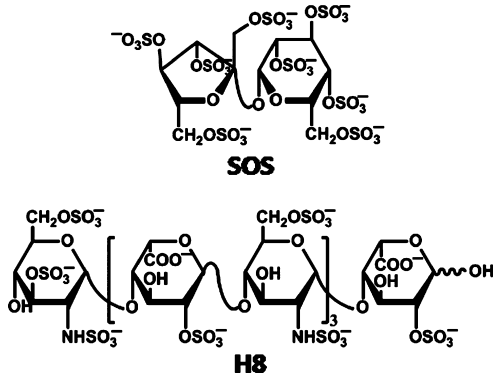

Figure 1. Structures of heparin octasaccharide H8 and sucrose octasulfate.

thus serve as a possible lead scaffold in structure-based drug design. We have characterized the equilibrium binding of SOS to active thrombin in solution and have studied its effects on thrombin's catalytic activity. We have parsed the contributions of ionic and hydrogen bond interactions to thrombin−SOS complex stabilization and find significant differences between it and that of the thrombin−heparin complex. Interestingly, SOS inhibits thrombin to a small extent and is thus the first carbohydrate-based inhibitor of this protease. We also determined the crystal structure of the SOS complex with BT, which shows that two SOS molecules bind in exosite II between the opposed carboxyl termini of the thrombin dimer that constitutes the asymmetric unit of the crystal lattice. This thrombin crystal dimer has a monomer association mode different from that observed in the PPACK-HT−LMWH complex.[28] A consequence of this difference is that one SOS molecule in the BT−SOS complex binds at the same locus as heparin in exosite II of HT through interactions almost exclusively with one BT monomer, while a second SOS binds at an adjacent locus, interacting with both exosite II portions of the juxtaposed BT monomers of the dimer. These studies provide evidence for distinctions in the mode and nature of SOS and heparin binding at exosite II of thrombin and in their effects on catalytic activity. Finally, they affirm the possibility of designing specific, small, synthetic allosteric inhibitors of thrombin targeted to exosite II.

EXPERIMENTAL PROCEDURES

Materials. Human and bovine α-thrombins were purchased from Haematologic Technologies, Inc. (Essex Junction, VT) as 10 mg/mL solutions in a glycerol/water (1:1, v/v) mixture. D-Phenylalanyl-L-prolyl-L-arginine chloromethyl ketone and SOS were purchased from Biomol International (now Enzo Life Sciences International, Inc., Plymouth Meeting, PA). Sodium heparin was from Arcos, and Spectrozyme TH was purchased from American Diagnostica (Greenwich, CT). Clinically used Lovenox (enoxaparin, Sanofi-Aventis) was purchased from the Virginia Commonwealth University Hospital pharmacy. Deionized distilled water (18.2 MΩ) from Fisher Scientific (Agawam, MA) was used to prepare all buffers. *p*-Aminobenzamidine was purchased from Sigma-Aldrich (St. Louis, MO), and other chemicals were from either Sigma-Aldrich or Fisher Scientific. All measurements, including the crystal structures, were taken at Na^+ concentrations far above that for saturation of the Na^+ binding site of thrombin.[29]

Thermodynamics of Thrombin Binding to SOS. The equilibrium dissociation constant (K_D) of the HT−SOS complex at 25 °C was measured in 20 mM sodium phosphate buffer (pH 7.4) containing 0.1 mM EDTA, 0.1% (w/v) PEG 8000, and varying concentrations of NaCl (50−250 mM). In this range of sodium concentrations, thrombin will be entirely in the high-sodium form. The active site binding probe, PABA, was used as a fluorescent reporter group for ligand binding at exosite II.[30,31] PABA binds noncovalently in the P1 specificity pocket of trypsin-like serine proteases, including thrombin. Although the P1 specificity pocket of thrombin lies on the opposite side of the thrombin molecule from exosite II, at a distance of ~25 Å, PABA bound in that pocket shows fluorescence changes on binding of heparin to exosite II. In the experiments described here, a subinhibitory concentration of PABA (10 μM) was used, well below its K_D of ~60−80 μM,[30] so that only a small fraction of thrombin molecules are bound. Fluorescence experiments were performed in PEG 20000-coated cuvettes using a QM4 spectrofluorometer (Photon Technology International, Birmingham, NJ) in ratio mode. The fluorescence of the HT−PABA complex (λ_{EM} = 370 nm; λ_{EX} = 345 nm) as a function of the addition of aliquots of SOS was measured with correction for dilution. SOS does not absorb significantly at either 345 or 370 nm, and hence, no inner filter corrections were necessary. The slit widths on the excitation and emission side were 1 and 2 mm, respectively. The decrease in the magnitude of the fluorescence signal due to SOS binding at exosite 2 was fitted to the quadratic equilibrium binding

equation (eq 1) to obtain the K_D of interaction:

$$\frac{\Delta F}{F_o} = \frac{\Delta F_{MAX}}{F_o}\left\{\left[[T]_o + [SOS]_o + K_D - \sqrt{([T]_o + [SOS]_o + K_D)^2 - 4[T]_o[SOS]_o}\right] / (2[T]_o)\right\} \quad (1)$$

where ΔF is the change in fluorescence relative to the initial fluorescence F_o on formation of the complex following each addition of SOS and ΔF_{MAX} is the maximal change in fluorescence observed upon saturation of thrombin ($[T]_o$). A binding stoichiometry of 1:1 was determined for the SOS–HT complex using stoichiometric titrations with PABA as a probe of interaction (data not shown). This stoichiometry is consistent with the crystal structure of the complex and with the analytical ultracentrifugation results.

The contribution of ionic and nonionic binding energy to HT–SOS interaction was derived from measurement of K_D in buffers of varying ionic strength using eq 2:[23,26,32,37]

$$K_{D,OBS} = K_{D,NI} + \Psi Z \times \log[Na^+] \quad (2)$$

In the absence of any added NaCl, the ionic strength (I) of the buffer is 0.035 at pH 7.4. Higher ionic strengths were achieved via addition of NaCl, whose concentration ranged from 50 to 250 mM for the measurements that were taken. In eq 2, $K_{D,NI}$ is the dissociation constant at 1 M Na^+; Z carries information about the number of charge–charge interactions, and Ψ is the fraction of monovalent counterions released per negative charge following binding of SOS to thrombin.

Direct Inhibition of Thrombin by SOS. The direct inhibition of HT and BT by SOS was assessed through a chromogenic substrate (Spectrozyme TH) hydrolysis assay, as previously described for sulfated lignins[17,18] and also adapted to a 96-well plate format performed on a microplate reader. In the former, a 1–10 μL sample of SOS was diluted with 20 mM sodium phosphate or 20 mM Tris buffer (pH 7.4) containing 150 mM NaCl, 0.1 mM $CaCl_2$ or 0.1 mM EDTA, and 0.1% (v/v) PEG 8000 at room temperature in a PEG 20000-coated polystyrene cuvette. A solution of either 0.5 or 1.0 μM α-thrombin was added followed either immediately or after incubation for 10 min at room temperature by addition of 15–50 μL of 1–2 mM Spectrozyme TH. The final volume of the assay was 1000 μL, and the final concentrations of α-thrombin and Spectrozyme TH were 5 nM and 50 μM, respectively. The initial rate of increase in absorbance at 405 nm was measured for up to 500 s. In the 96-well plate format, 187 μL of a solution of SOS in 20 mM phosphate buffer (pH 7.4), 150 mM NaCl, 0.1 M EDTA, and 0.1% PEG 8000 was incubated with 5 μL of 500 nM thrombin at 25 °C in wells of a 96-well plate for 10 min. Following incubation, 8 μL of 1 mM Spectrozyme TH was added, and the initial change in absorbance at 405 nm was measured (final concentrations of thrombin and Spectrozyme TH were 12.5 nM and 40 mM, respectively). The fractional thrombin activity at each concentration of SOS was calculated using the activity measured under otherwise identical conditions in the absence of SOS. Logistic eq 3 was used to fit the dose dependence of relative thrombin activity to obtain the IC_{50}:

$$Y = Y_o + \frac{Y_M - Y_o}{1 + 10^{(\log[SOS]_o - \log IC_{50})\times HS}} \quad (3)$$

where Y is the ratio of thrombin activity in the presence of SOS to that in its absence, Y_M and Y_0 are the maximum and minimum possible values of fractional thrombin activity, respectively, IC_{50} is the concentration of SOS that results in 50% inhibition of thrombin, and HS is the Hill slope. Sigmaplot 8.0 (SPSS, Inc., Chicago, IL) was used to perform nonlinear curve fitting in which Y_M, Y_o, IC_{50}, and HS were allowed to float.

Inhibition by SOS of Cleavage of Fibrinogen by Thrombin. The inhibition of HT cleavage of fibrinogen by SOS was measured in a turbidimetric assay, as previously described for sulfated lignins.[33] A 48 μL sample of SOS was diluted with 950 μL of 20 mM sodium phosphate (pH 7.4) containing 40 mg/mL human fibrinogen, 100 mM NaCl, 0.1 mM EDTA, and 0.1% (v/v) PEG 8000 at room temperature in a PEG 20000-coated polystyrene cuvette. Two microliters of 2.65 μM human α-thrombin was added, and the increase in turbidity at 600 nm was measured immediately for up to 300 s.

Competitive Binding Studies with Low-Molecular Weight Heparin and SOS. Inhibition of thrombin by SOS was performed in the presence of 50 μM LMWH using the 96-well plate format. A 192 μL solution of SOS and thrombin with 50 μM LMWH in 20 mM phosphate buffer (pH 7.4) containing 150 mM NaCl, 0.1 mM EDTA, and 0.1% PEG 8000 was incubated at 25 °C for 10 min. Following incubation, 8 μL of 1 mM Spectrozyme TH was added and the initial change in absorbance at 405 nm measured. A thrombin concentration of 12.5 nM was found to give sufficient signal at various concentrations of the chromogenic peptide for reproducible results. The dose dependence of the fractional residual proteinase activity at each concentration of the competitor was fitted by eq 3 to obtain the apparent concentration of SOS required to reduce thrombin activity to 50% of its initial value ($IC_{50,app}$). Quantitative comparison of competitive binding was performed using the Dixon–Webb relationship (eq 4). In this equation, K_{LMWH} is the dissociation constant of the thrombin–LMWH complex, which has been reported to be ~60 μM.[23]

$$IC_{50,app} = IC_{50}\left(1 + \frac{[LMWH]_o}{K_{LMWH}}\right) \quad (4)$$

Thrombin–SOS Crystal Structure Studies. BT was exchanged into 10 mM Tris (pH 8.0) and 50 mM NaCl by repeated dilutions and concentration in an Amicon YM-10 centrifugal concentrator. Aliquots of 10 μL were stored at −80 °C and diluted to 7 g/L with the same buffer at the time of use. The BT–SOS complex was formed by incubation of 20 mM SOS with BT at 7 mg/mL for 1 h. This incubated solution was then set to crystallize in hanging drops under conditions optimized from those described by Iyaguchi et al.[34] A 4 μL drop of BT–SOS incubation solution was mixed with 4 μL of precipitant reservoir solution consisting of 0.1 M sodium citrate (pH 6.2), 20% (w/v) PEG 3350, and 15% (v/v) 2-propanol and equilibrated against the reservoir solution at room temperature. Isometric crystals of 0.5 mm grew under these conditions and diffracted to 2.2 Å resolution. An identical crystal form was obtained with 1 mM $CaCl_2$ added to the precipitant under otherwise identical conditions. These latter

Table 1. Crystallographic Data Collection and Refinement

	3PMB	3PMA
Data Collection		
resolution (Å)	39.2−2.80 (3.00−2.90)	29.72−2.20 (2.28−2.20)
$I/\sigma(I)$ (highest-resolution shell)	7.2 (4.4)	13.5 (6.2)
% completeness (highest-resolution shell)	84.6 (6.6)	99.8 (100.0)
N_{obs}	14843	38669
multiplicity (highest-resolution shell)	4.19 (4.62)	7.88 (9.04)
R_{merge} (highest-resolution shell)	0.158 (0.314)	0.083 (0.311)
Refinement		
resolution (Å)	15.0−2.90 (2.97−2.90)	27.8−2.20 (2.26−2.20)
R_{work} (highest-resolution shell)	0.242 (0.289)	0.204 (0.267)
R_{free} (highest-resolution shell)	0.301 (0.368)	0.245 (0.327)
N_{work}	13968	36728
N_{free}	746	1938
N_{atoms}	4514	4904
$\langle B_{protein} \rangle$	33.4	44.8
$\langle B_{water} \rangle$	11.9	31.4
$\langle B_{ligand} \rangle$	29.6	84.2
rmsd from ideal		
bond lengths (Å)	0.01	0.008
bond angles (deg)	1.23	1.24
Ramachandran plot		
no. of residues in most favored regions	396	410
no. of residues in additionally allowed regions	63	59
no. of residues in generously allowed regions	2	
no. of residues in forbidden regions		1

crystals were back-soaked stepwise into the same precipitant solution in which the citrate buffer was replaced with bis-Tris to minimize possible competitive effects of citrate on SOS binding. These crystals diffracted to 2.4 Å resolution. Diffraction intensity data were collected without further cryoprotection from crystals at 100 K on a Rigaku Micromax 007a instrument with Varimax confocal optics and an RAXIS IV^{++} detector over 180° in Φ in 0.5° steps. Intensity data were integrated, scaled, and merged using d*trek and converted to amplitudes with TRUNCATE in the CCP4 program suite. The space group was inferred to be $P4_32_12$, the same as that of the unliganded BT crystals obtained under these conditions. (The unliganded BT crystals diffracted to only 3.2 Å resolution and had one lattice dimension significantly longer than that of the SOS-complexed thrombin crystals.) The Matthews coefficient indicated two molecules of BT per asymmetric unit. A molecular replacement solution was found using PHASER 2.1 and the coordinates of the BT light and heavy chains from RCSB Protein Data Bank (PDB) entry 1MKX as a search model. The model was initially refined via Cartesian simulated annealing using Phenix.refine and then further refined by alternating cycles of manual fitting in COOT and computational refinement in REFMAC. Statistics for the final refined model structure are listed in Table 1. Coordinates and structure factors for the unliganded BT and SOS−BT crystal structures have been deposited in the Protein Data Bank as entries 3PMB and 3PMA, respectively.

Analytical Ultracentrifugation of Thrombin−SOS and Thrombin−Heparin Complexes. BT was diluted to 1.2 mg/mL in 10 mM Tris-HCl buffer (pH 8) and 50 mM NaCl and human thrombin to 0.5 mg/mL in the same buffer. Samples (420 μL) of thrombin alone and thrombin with 20 mM SOS, equimolar LMWH, or equimolar unfractionated heparin (UFH) with a buffer sample were run at 45000 rpm overnight at 20 °C in a Beckman Coulter Proteome Lab XL-I analytical ultracentrifuge. Absorbance and interference scans were recorded until the boundary moved to the bottom of the cell. The continuous distribution $c(M)$ analysis was performed using SEDFIT (https://sedfitsedphat.nibib.nih.gov). $S_{20,w}$ values were calculated for various oligomer complexes from the crystal structures of the PPACK-HT−LMWH complex (PDB entry 1XMN) and the BT−SOS complex using Hydropro version 7.c.[35]

RESULTS

Thrombin Binds to SOS with High Affinity. To test whether SOS associates with thrombin, we used a fluorimetric method similar to that used for measuring the affinity of heparin for thrombin.[30] In the original method, the interaction of heparin in exosite II of thrombin decreases the fluorescence of the noncovalent, active site-bound PABA probe in a saturable manner, which can be fitted by the quadratic binding eq 1 to obtain a K_D. The interaction of SOS with exosite II of HT resulted in a maximal decrease in fluorescence at 370 nm of approximately 5% in 20 mM sodium phosphate buffer (pH 7.4) containing 50 mM NaCl, 0.1 mM EDTA, and 0.1% PEG 8000 (Figure 2A).

This maximal decrease was less than that measured for heparin (∼13−17%) but was consistent and independent of the concentration of thrombin used in the experiment. Fitting eq 1 to the data gave a K_D of 1.4 μM, which is remarkably close to that measured for full-length heparin (1.45 μM) under identical conditions (pH 7.4, I = 0.085, 25 °C).[23] The affinity corresponds to a free energy of binding of 7.9 kcal/mol

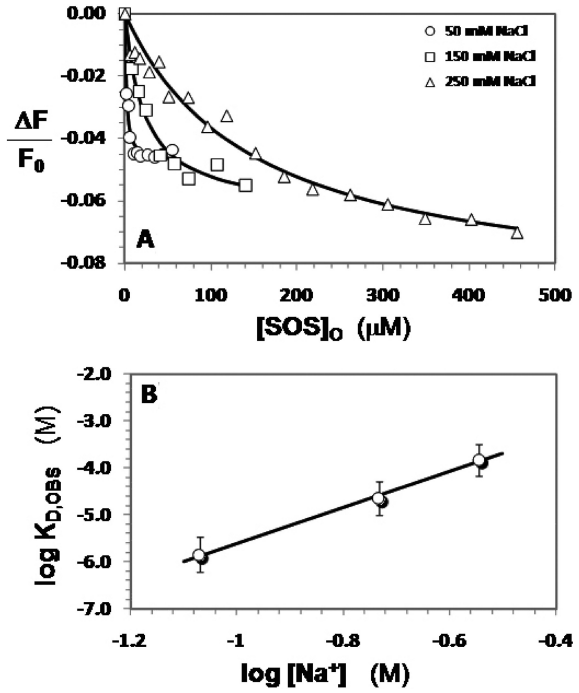

Figure 2. (A) Interaction of SOS with human thrombin at pH 7.4 and 25 °C in the presence of 50 (○), 150 (□), and 250 mM NaCl (△). The decrease in fluorescence of the bound external probe, PABA (λ_{EX} = 345 nm; λ_{EM} = 370 nm), that accompanies binding of SOS was used to calculate the $K_{D,OBS}$ of the SOS−thrombin complex. Solid lines represent nonlinear fits to the data using quadratic eq 1. (B) Dependence of $K_{D,OBS}$ on the ionic strength of the medium at pH 7.4. The solid line represents a linear regression fit using eq 2.

Table 2. Interaction of SOS with Human α-Thrombin at pH 7.4 and 25 °C

	$K_{D,OBS}$ (μM)[a]	ΔF_{MAX} (%)[a]	$\Delta G°$ (kcal/mol)
50 mM NaCl	1.4 ± 0.3[b]	−4.8 ± 0.1	7.9 ± 0.1
150 mM NaCl	22 ± 4	−6.4 ± 0.3	6.4 ± 0.2
250 mM NaCl	149 ± 25	−9.2 ± 0.6	5.2 ± 0.2

[a]Measured spectrofluorometrically using a saturable decrease in fluorescence (λ_{EM} = 370 nm) of PABA due to the binding of SOS to thrombin. See Experimental Procedures for details. [b]Errors represent one standard error.

(Table 2), suggesting a surprisingly high-affinity interaction for such a small disaccharide structure. Similar measurements with BT, for which the crystal structure with SOS was determined, gave a comparable K_D of 4.0 ± 0.4 μM (data not shown).

The High Affinity of SOS for Thrombin Originates from Multiple Ionic Interactions. To determine the nature of the interactions of SOS with HT, the dissociation constant ($K_{D,OBS}$) was measured as a function of NaCl concentration. According to the protein−polyelectrolyte theory,[23,30] log-[$K_{D,OBS}$] is linearly dependent on log[Na^+] with an intercept of log $K_{D,NI}$ (see eq 2), where $K_{D,NI}$ is the equilibrium dissociation constant due to nonionic forces. This relationship provides the binding energy due to ionic forces ($\Delta G°_{IONIC}$) from the slope and that due to nonionic forces ($\Delta G°_{NON-IONIC}$) from the intercept of the linear plot.

The affinity of thrombin for SOS at several salt concentrations was measured fluorimetrically, as described above. In all cases, the maximal change in fluorescence was consistently in the range of 5−8% (Figure 2A). The log $K_{D,OBS}$ increased linearly with log[Na^+] at pH 7.4 for the HT−SOS interaction (Figure 2B). The slope of this line was calculated to be 3.8 ± 0.5 versus a slope of 4.8 ± 0.2[23] for full-length heparin, indicating similar ionic interactions of the two polyanions. This corresponds to an ionic binding energy of 4.5 kcal/mol under physiological conditions (pH 7.4, I = 0.15, 25 °C). Full-length heparin was found to make approximately six ionic interactions (5.8 ± 0.2) with HT,[26] which corresponds to an ionic binding energy of 5.7 kcal/mol. The comparable ionic binding energies of SOS and heparin to HT indicate that these two ligands make a similar number of ionic bonds in their complexes.

The intercept (log $K_{D,NI}$) of the linear plot for binding of SOS to HT was found to be −1.8 ± 0.4 (Figure 2B). This corresponds to a $K_{D,NON-IONIC}$ of 16.6 ± 6.3 mM, which implies a contribution of 2.4 kcal/mol due to nonionic forces. This contribution of nonionic forces to the binding affinity of SOS for HT calculates to approximately 35% of the total binding energy at physiological ionic strength (pH 7.4, I = 0.15), a substantial contribution that most probably arises from multiple hydrogen bonds. In comparison, the nonionic affinity of full-length heparin was measured to be 200 ± 100 mM, suggesting a much smaller contribution of nonionic forces to the heparin−HT complex[31] than the SOS−HT complex. This implies that the SOS−HT complex is characterized by an approximately 12.5-fold higher nonionic contribution than the heparin−HT complex.[23]

SOS Inhibits Thrombin with High Potency but Weak Efficacy. Although heparin binding to exosite II results in a change in the fluorescence properties of PABA bound in the active site of thrombin, heparin is not a direct (antithrombin-independent) thrombin inhibitor. It has been reported that SOS weakly (≤10%) inhibits thrombin hydrolysis of CBS31.39 (CH_3SO_2-D-Leu-Gly-Arg-*p*-nitroanilide),[27] and we have further tested this effect using a different substrate. Thrombin activity was measured under pseudo-first-order conditions in 20 mM sodium phosphate or 20 mM Tris buffer (pH 7.4, I = 0.15, 25 °C) in a spectrophotometric assay using Spectrozyme TH substrate, as previously performed for sulfated lignins.[17,18] As the concentration of SOS increased, the proteolytic activity decreased in a sigmoidal manner (on a semilog plot) (Figure 3A). This decrease could be fitted using the sigmoidal dose dependence (eq 3) to derive an IC_{50} of 4.5 ± 1.1 μM with a Hill slope of 1.5 ± 0.5. For an allosteric, noncompetitive inhibitor, the IC_{50} correlates well with the inhibition constant (K_I), and therefore, this result suggests that SOS is a fairly potent inhibitor of thrombin. Considering that most GAG-binding sites are surface-exposed and shallow and are not conducive to high affinity, the low micromolar potency of a small, highly sulfated molecule, SOS, is striking.

To test whether the ability to inhibit thrombin hydrolysis of small chromogenic substrates translates into the ability to inhibit cleavage of macromolecular substrates, we measured thrombin cleavage of human plasma fibrinogen in the presence of SOS. Fibrinogen cleavage results in the formation of polymeric fibrin, which reduces transmittance at 600 nm. Fibrinogen cleavage profiles measured in the presence of 0.7−1.8 mM SOS show a gradual increase in the lag time of cleavage (Figure 3B), suggesting that SOS inhibits the thrombin-catalyzed fibrinogen cleavage reaction.

dx.doi.org/10.1021/bi2004526 | *Biochemistry* 2011, 50, 6973−6982

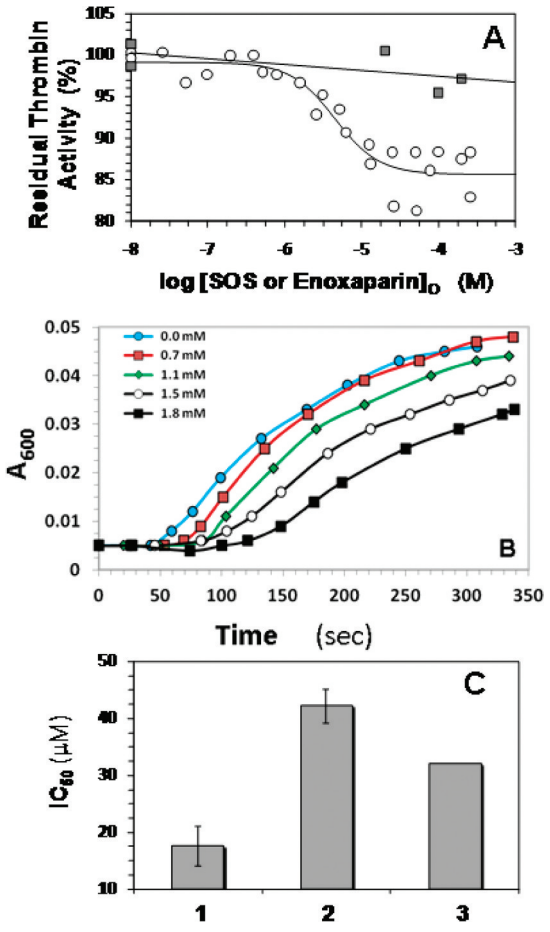

Figure 3. (A) Direct inhibition of human α-thrombin by SOS or enoxaparin. The assay mixture consisted of 20 mM sodium phosphate or Tris-HCl buffer (pH 7.4) containing 150 mM NaCl, 0.1% PEG 8000, and either 0.1 mM EDTA or 0.1 mM $CaCl_2$ at 25 °C. Thrombin inhibition was measured spectrophotometrically using the Spectrozyme TH hydrolysis assay: (○) SOS and (■) enoxaparin. For the SOS data, the solid line represents the dose–response fit that yields IC_{50} and the Hill slope (eq 3), as described in Experimental Procedures. For the enoxaparin data, the solid line is a linear trend line. (B) Cleavage of fibrinogen by thrombin in the presence of SOS. The inhibition of HT cleavage of fibrinogen by SOS was followed via time-dependent turbidimetric measurements at 600 nm of thrombin-catalyzed cleavage of a 40 mg/mL sample of human fibrinogen at different SOS concentrations, as described in Experimental Procedures. (C) Competitive binding of SOS and enoxaparin to human α-thrombin. Thrombin was inhibited in the presence of 50 μM enoxaparin in a manner similar to that in its absence, and the resulting data were fitted by the dose–response equation to yield the apparent IC_{50}: (1) SOS alone, (2) SOS and 50 μM enoxaparin, and (3) IC_{50} predicted by the Dixon–Webb relationship for ideal competitive binding. Error bars represent one standard error. See the text for details.

Despite the high potency of thrombin inhibition, the Y_o and Y_M for inhibition of Spectrozyme TH hydrolysis calculated from eq 3 indicate a maximal inhibition of only 13.5 ± 0.2% for HT (Figure 3A) and 20 ± 2.0% for BT (not shown). This implies that the efficacy of thrombin inhibition by SOS is weak, but still significant, and contrasts with that of heparin (full-length or LMWH), which does not inhibit the enzyme even at concentrations as high as 200 μM.[18]

SOS Competes with Low-Molecular Weight Heparin for Interaction with Human Thrombin. If SOS binding in exosite II of thrombin is the source of thrombin inhibition, then it is expected to compete with full-length heparin or LMWH and show a decrease in the potency of thrombin inhibition. Competition studies were performed by monitoring thrombin's proteolytic activity as a function of SOS in the presence of a fixed concentration of LMWH. In the presence of 50 μM LMWH, the IC_{50} increased to 42 ± 3 μM (Figure 3C). Furthermore, the presence of LMWH did not affect the efficacy of SOS inhibition of thrombin, which remained unchanged at ~11%. According to the Dixon–Webb relationship for ideal competitive behavior, the apparent IC_{50} expected for SOS is 32 μM, very close to that observed. The decrease in the level of inhibition of thrombin by SOS in the presence of LMWH confirms that SOS binds at exosite II and that this binding is the source of the inhibition of catalytic activity.

SOS Binds at Two Nonequivalent Subsites of Exosite II in the Monomer–Monomer Interface of a Bovine Thrombin Dimer. The crystal structure of the BT–SOS complex shows binding of two SOS molecules at the interface of the two BT monomers constituting the crystallographic asymmetric unit. The BT dimer in this crystal lattice is not the same as that for PPACK-HT in its crystal structure with LMWH.[28] Figure 4 shows the distinct monomer–monomer association mode of the BT–SOS complex compared to that of the PPACK-HT–LMWH complex. One monomer of each of these dimer structures was superposed (HT2 and BT2, bottom, pale green), and the relative positions of the other monomers in each of the dimer structures are colored pink (PPACK-HT–LMWH complex) and wheat (BT–SOS complex). In the PPACK-HT–LMWH structure, the exosite II portions (blue) of the two HT monomers (pink and light green) in the dimer are almost exactly juxtaposed. The LMWH (red stick) binds in this interface, and the local 2-fold rotation axis relating the two HT monomers approximately bisects the LMWH (red stick) bound between them. In the BT–SOS complex (wheat and light green), the exosite II portions (blue) of the opposed monomers are not exactly juxtaposed across the dimer interface but are skewed so that only parts of the exosites face each other. This skewing of the two BT monomers leaves much of exosite II on each BT monomer open for unimpeded SOS (green sticks) binding, resulting in two nonequivalent binding sites per BT dimer (sites A and B).

The thrombin ligand groups that interact with the sulfate groups of SOS are listed in Table 3, and a detailed comparison of the interactions of BT and HT with SOS and LMWH, respectively, is shown in panels A and B of Figure 5. The binding of SOS in site A is almost exclusively to charged residues in exosite II of a single BT monomer (Figure 4, light green monomer; Figure 5A, residues labeled in black) and suggests that polyanion binding to this site does not require a thrombin dimer for complex formation. The second SOS ligand in site B makes fewer interactions with BT, and these are approximately equally distributed between the two thrombin monomers (Figure 4, light green and wheat) in the dimer (Figure 5B). The close approach of two sulfate groups, one from each of the two bound SOS molecules, is stabilized by the intervening ε-amino group of K240. Both sites are inferred to be simultaneously occupied, because the refined occupancies of each of the SOS ligands are 0.75–0.80. Three of the residues (K87, K235, and R244) that interact with SOS in site B do not interact with LMWH in its complex with PPACK-HT (magenta), though they lie in the zone

dx.doi.org/10.1021/bi2004526 | Biochemistry 2011, 50, 6973–6982

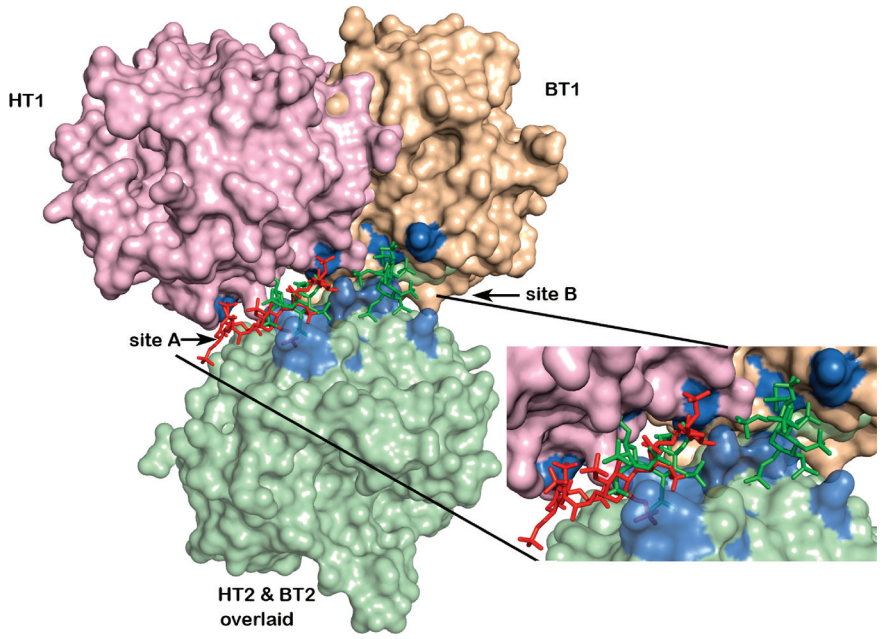

Figure 4. Differences in monomer contacts between HT−LMWH complex and BT-SOS complex dimers. Monomer AB (HT2) of the AB−GH dimer of the HT−heparin complex was superposed on monomer CD (BT2) of the AB−CD dimer of the BT−SOS complex (light green surface). The relative positions after this superposition of the monomer mates [GH (HT1) in the HT−heparin complex and AB (BT1) in the BT−SOS complex] in each of the dimers are colored pink and wheat, respectively. LMWH (red stick) bound to the HT−LMWH dimer and SOS (green stick) bound to sites 1 and 2 of the BT−SOS complex are shown after superposition of HT2 and BT2 monomers. Both ligands occupy the extended exosite II (residue surface colored blue) shown as a close-up.

Table 3. Thrombin Amino Acid Residues That Interact with Sulfate Groups of Heparin and SOS in Their Crystal Complexes

	K87	H91	R93	R101	R/K126	R165	R233	K235	K236	W237	K240	R244
Heparin – HT		√	√	√	√	√	√		√	√	√	
SOS – BT	√	√	√	√	√			√	√	√	√	√

√ amino acid interacts with sulfate group in crystal complex

amino acid does not interact with sulfate group in crystal complex

Binding of SOS at site B of a thrombin monomer would likely be weaker than that for binding to site A, because of the smaller number of interactions between SOS and either of the two monomers that contribute to its binding site.

The 4−5 ionic interactions between SOS and BT in exosite II (site A) of the crystal structure complex are consistent with multiple ionic interactions calculated from solution binding data. There are several other defined cationic side chains that could be reoriented to make interactions with sulfates of SOS but instead adopt alternative conformations. These may be restrained by interactions with solvent molecules, not all of which could be confidently placed at the resolution of our electron density map.

The crystal lattice of unliganded BT, crystallized under the same conditions from which the BT−SOS complex crystallized, is closely similar to that of the latter, differing by 7 Å along one lattice direction. This implies that the mode of dimerization in the BT−SOS crystals is not due to differences between SOS and LMWH, or the irreversible inhibition of HT by PPACK in its complex with LMWH. Rather, it is more likely a consequence of the small differences in crystallization conditions, possibly specific to each thrombin, despite their high degree of sequence similarity (86% identical and 92% similar).

Analytical Ultracentrifugation. Crystals of HT−LMWH and BT−SOS complexes were obtained under nonphysiological conditions. To determine the relationship between the oligomeric modes of thrombin-ligand complexes observed in the crystal structures and those that exist under more physiological conditions in solution, we determined the profile of molecular species in these thrombin−ligand mixtures by analytical ultracentrifugation and used the known structures of the crystal complexes to calculate expected $S_{20,w}$ values (Figure 6).

Sedimentation velocity ultracentrifugation was conducted on BT and HT alone and incubated with SOS and heparin in 10 mM Tris-HCl buffer (pH 8) and 50 mM NaCl at high (1.2 mg/mL) concentrations of BT and lower (0.5 mg/mL) concentrations of HT to check for concentration-dependent aggregation. In the presence and absence of the SOS ligand, BT and HT had $S_{20,w}$ values of 3.1−3.2. This is in agreement with the $S_{20,w}$ value (3.14) calculated for the thrombin monomers

dx.doi.org/10.1021/bi2004526 | *Biochemistry* 2011, 50, 6973−6982

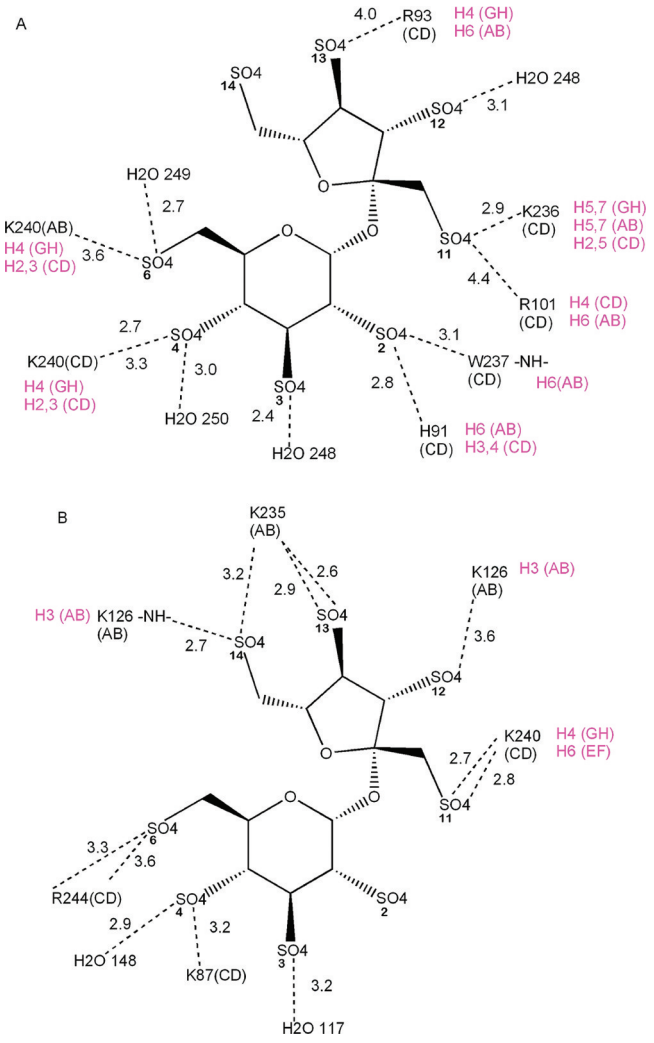

Figure 5. Schematic diagram of the interactions (dotted lines) of each of the two SOS ligands with groups on BT in (A) site 1 and (B) site 2. Distances are shown in angstroms. The thrombin monomer of each interacting group is denoted in black by AB or CD. Double lines from a single group indicate that two possible hydrogen bonds could form simultaneously for the indicated pair. Magenta denotes the heparin subunit (H prefix) in the HT−LMWH complex structure to which the indicated residue binds and the thrombin chain in which the residue occurs.

from their crystal structures. The slight shift in the mobility of the BT−SOS peak relative to that of BT alone is consistent with formation of a monomeric BT−SOS complex. In contrast, deconvolution of the broad peak observed for the LMWH complex with BT shows three species. These are consistent with monomer (3.45), dimer (4.45), and tetramer (5.5) complexes of BT with LMWH. The profile of the HT−LMWH complex (not shown) shows only a species with an $S_{20,w}$ of 4, which is most consistent with a 2:1 HT−LMWH dimer, similar but not identical to that observed in the crystal structure of this complex, from which an $S_{20,w}$ of 4. 72 is calculated.[28] This difference may indicate a difference in the frictional ratio between the complex in solution and that in the crystal structure, or it may arise from the fact that the crystal complex was composed of PPACK-inhibited HT and LMWH.

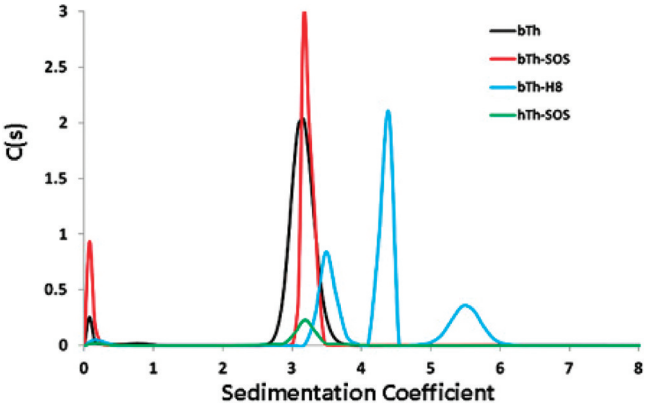

Figure 6. Sedimentation velocity profile showing molecular species of thrombin−ligand complexes. $C(s)$ is the relative concentration of each species: black for unliganded BT, red for the BT−SOS complex, green for the HT−SOS complex, and blue for the BT−LMWH complex.

DISCUSSION

The high affinity of thrombin for full-length heparin has been attributed to the fact that the polysaccharide is a linear molecule of nearly 10−30 disaccharides that represent millions of sequences (Figure 1). This increases the probability of favorable electrostatic interaction with a high-affinity subset of this large population. The probability of interaction is further increased because heparin contains a large number of iduronic acid residues, which confer conformational flexibility ($^1C_4$ and ^2S_O forms) on the polymer.

In contrast to heparin, SOS is considerably smaller and homogeneous with a much more limited distribution of conformations. For these reasons, it was expected that SOS would have a low-affinity interaction with exosite II of thrombin. It is therefore surprising that SOS, a molecule ∼15-fold smaller than full-length heparin, binds to human thrombin with nearly identical affinity and with a greater nonionic energy contribution. This suggests that SOS has some structural features and charge properties that distinguish it from heparin and could confer tight binding to thrombin. Nonionic binding energy in interactions of sulfate groups is likely to arise from the partial hydrogen bond character of the primarily electrostatic sulfate−arginine (or lysine) ion pairs. This hydrogen bond character increases the specificity of interaction because of its directionality[36] and could confer a greater specificity on the interaction of SOS with thrombin than is observed for heparin, whose interactions with thrombin are predominantly ionic.

At least 10 unique crystal structures of SOS−protein complexes have been determined (PDB entries 1AFC, 1LR7, 2P39, 2UWN, 2UUS, 2V5E, 3CU1, 3LDJ, 3K6B, and 3QRC), but none for thrombin with SOS. The BT−SOS crystal structure described here appears to have a single mode of SOS binding with two SOS molecules bound at the monomer−monomer interface of the thrombin crystal dimer. This 1:1 stoichiometry and the disposition of the two thrombin monomers in the BT−SOS crystal dimer differ from those of the HT−LMWH complex whose stoichiometry is 1:2 (LMWH:HT). The two exosite II portions of the HT−LMWH complex sandwich the single LMWH, which lies centered on the noncrystallographic 2-fold axis relating the two HT monomers. The SOS bound in site A of the BT−SOS complex interacts with a large fraction of the same anionic groups with which LMWH interacts in the

dx.doi.org/10.1021/bi2004526 | *Biochemistry* 2011, 50, 6973−6982

exosite II portions of the HT crystal dimer. However, in the BT−SOS complex, these groups, with one exception, are entirely on a single thrombin monomer, in contrast to the HT−LMWH complex, where they are contributed by both thrombin monomers in the dimer. The exception is K240, which lies between proximal sulfate groups of the two adjacent SOS ligands bound in the exosite II portions of the BT crystal dimer. The analytical ultracentrifugation results are consistent with the crystal structures, showing 1:1 SOS−BT and SOS−HT complexes and a 1:2 LMWH−HT complex.

The reduction in thrombin's ability to hydrolyze small peptides as a result of its interaction with SOS distinguishes this polyanion ligand from heparin, which does not show this effect. Our measurements show a lower K_D for SOS binding to thrombin and somewhat higher levels of thrombin inhibition by SOS than have been reported by others.[27] These differences may be due to use of different buffer conditions (ionic strength and presence of Ca^{2+}) and/or different substrates.

There are several possible ways in which SOS binding could alter the activity of thrombin. The higher specificity in the SOS interaction conferred by a greater contribution of nonionic forces to stabilization of the SOS−thrombin complex may impose a specific local conformation that affects the active site through altered static or dynamic properties of the protein. The available structures of BT and the BT−SOS complex are not of sufficient resolution to reveal subtle static changes in structure that could be responsible for this modest loss of thrombin activity on binding SOS, but any such changes are extremely limited. Alternatively, the higher specificity of the interaction of SOS with thrombin may alter the dynamics of the thrombin structure and/or the population distribution of active thrombin conformers, which manifests as allostery.[37−39] Possibly related to such dynamics-driven allostery is the displacement of solvent on binding of heparin and SOS to exosite II. Although SOS has a higher charge density than heparin, heparin binding to thrombin may displace less bound water than SOS because of the presence of hydroxyl groups on heparin and their absence on SOS. Such solvent effects could contribute to the higher affinity of SOS for thrombin compared to the affinity of heparin for thrombin. Finally, the difference in the solution oligomeric state of thrombin between the SOS complex (monomer) and the thrombin−LMWH complex (dimer) could also induce dynamic allosteric effects. The closed dimer of thrombin with LMWH may stabilize the two thrombin structures and suppress small structural changes necessary for inhibition of thrombin activity. The inhibition of thrombin catalytic activity by SOS binding in exosite II opens new possibilities for understanding communication between exosite II and the active site and also validates exosite II as a target for the design of more effective thrombin inhibitors.

AUTHOR INFORMATION

Corresponding Author

*E-mail: xrdproc@vcu.edu. Telephone: (804) 828-6139. Fax: (804) 827-3664.

Funding

This work was supported by grants from the National Institutes of Health (HL099420 and HL090586) and the American Heart Association (EIA 0640053N). Crystallography and computational infrastructure was provided by the Virginia Commonwealth University Structural Biology Core Facility, supported in part with funding from NIH-NCI Cancer Center Core Support Grant P30 CA016059.

ACKNOWLEDGMENTS

We thank Dr. Carlos Escalante for his generous help with the analytical ultracentrifugation experiments.

ABBREVIATIONS

HT, human thrombin; BT, bovine thrombin; LMWH, low-molecular weight heparin; MOPS, 3-morpholinopropane-1-sulfonic acid; PABA, *p*-aminobenzamidine; PAR, protease-activated receptor; PEG, polyethylene glycol; PPACK, D-phenylalanyl-L-prolyl-L-arginine chloromethyl ketone; SOS, sucrose octasulfate.

REFERENCES

(1) DiCera, E. (2008) Thrombin. *Mol. Aspects Med. 29*, 203−254.

(2) Crawley, J. T. B., Zanardelli, S., Chion, C. K. N. K., and Lane, D. A. (2007) The central role of thrombin in hemostasis. *J. Thromb. Haemostasis 5*, 95−101.

(3) Davie, E. W., and Kulman, J. D. (2006) An overview of the structure and function of thrombin. *Semin. Thromb. Hemostasis 32*, 3−15.

(4) Huntington, J. A. (2005) Molecular recognition mechanisms of thrombin. *J. Thromb. Haemostasis 3*, 1861−1872.

(5) Coughlin, S.R. (2005) Protease-activated receptors in hemostasis, thrombosis and vascular biology. *J. Thromb. Haemostasis 3*, 1800−1814.

(6) Brass, L. F. (2003) Thrombin and platelet activation. *Chest 124*, 18S−25S.

(7) Colognato, R., Slupsky, J. R., Jendrach, M., Burysek, L., Syrovets, T., and Simmet, T. (2003) Differential expression and regulation of protease-activated receptors in human peripheral monocytes and monocyte-derived antigen-presenting cells. *Blood 102*, 2645−2652.

(8) Moller, T., Weinstein, J. R., and Hanisch, U. K. (2006) Activation of microglial cells by thrombin: Past, present, and future. *Semin. Thromb. Hemostasis 32*, 69−76.

(9) Li, X., Syrovets, T., Paskas, S., Laumonnier, Y., and Simmet, T. (2008) Mature dendritic cells express functional thrombin receptors triggering chemotaxis and CCL18/pulmonary and activation-regulated chemokine induction. *J. Immun. 181*, 1215−1223.

(10) Chen, D., and Dorling, A. (2009) Critical roles for thrombin in acute and chronic inflammation. *J. Thromb. Haemostasis 7*, 122−126.

(11) Bunnett, N. W. (2006) Protease-activated receptors: How proteases signal to cells to cause inflammation and pain. *Semin. Thromb. Hemostasis 32*, 39−48.

(12) Esmon, C. T. (2003) The protein C pathway. *Chest 124*, 26S−32S.

(13) Ruf, W., and Mueller, B. M. (2006) Thrombin generation and the pathogenesis of cancer. *Semin. Thromb. Hemostasis 32*, 61−68.

(14) Bode, W. (2006) The structure of thrombin: A janus-headed proteinase. *Semin. Thromb. Hemostasis 32*, 16−31.

(15) Ye, J., Liu, L. W., Esmon, C. T., and Johnson, A. E. (1992) The fifth and sixth growth factor-like domains of thrombomodulin bind to the anion-binding exosite of thrombin and alter its specificity. *J. Biol. Chem. 267*, 11023−11028.

(16) Ye, J., Rezaie, A. R., and Esmon, C. T. (1994) Glycosaminoglycan contributions to both protein C activation and thrombin inhibition involve a common arginine-rich site in thrombin that includes residues arginine 93, 97, and 101. *J. Biol. Chem. 269*, 17965−17970.

(17) Monien, B. H., Henry, B. L., Raghuraman, A., Hindle, M., and Desai, U. R. (2006) Novel chemo-enzymatic oligomers of cinnamic

acids as direct and indirect inhibitors of coagulation proteinases. *Bioorg. Med. Chem. 14*, 7988−7998.

(18) Henry, B. L., Monien, B. H., Bock, P. E., and Desai, U. R. (2007) A novel allosteric pathway of thrombin inhibition. *J. Biol. Chem. 282*, 31891−31899.

(19) Liu, L. W., Vu, T. K., Esmon, C. T., and Coughlin, S. R. (1991) The region of the thrombin receptor resembling hirudin binds to thrombin and alters enzyme specificity. *J. Biol. Chem. 266*, 16977−16980.

(20) Hortin, G. L., and Trimpe, B. L. (1991) Allosteric changes in thrombin's activity produced by peptides corresponding to segments of natural inhibitors and substrates. *J. Biol. Chem. 266*, 6866−6871.

(21) Hogg, P. J., and Jackson, C. M. (1990) Formation of a ternary complex between thrombin, fibrin monomer, and heparin influences the action of thrombin on its substrates. *J. Biol. Chem. 265*, 248−255.

(22) Hogg, P. J., Jackson, C. M., Labanowski, J. K., and Bock, P. E. (1996) Binding of fibrin monomer and heparin to thrombin in a ternary complex alters the environment of the thrombin catalytic site, reduces affinity for hirudin, and inhibits cleavage of fibrinogen. *J. Biol. Chem. 271*, 26088−26095.

(23) Olson, S. T., Halvorson, H. R., and Björk, I. (1991) Quantitative characterization of the thrombin-heparin interaction. Discrimination between specific and nonspecific binding models. *J. Biol. Chem. 266*, 6342−6352.

(24) Verhamme, I. M., Olson, S. T., Tollefsen, D. M., and Bock, P. E. (2002) Binding of exosite ligands to human thrombin. *J. Biol. Chem. 277*, 6788−6798.

(25) Vacca, J. P. (2000) New advances in the discovery of thrombin and factor Xa inhibitors. *Curr. Opin. Chem. Biol. 4*, 394−400.

(26) Srivastava, S., Goswami, L. N., and Dikshit, D. K. (2005) Progress in the design of low molecular weight thrombin inhibitors. *Med. Res. Rev. 25*, 66−92.

(27) Sarilla, S., Habib, S. Y., Kravtsov, D. V., Matafonov, A., Gailani, D., and Verhamme, I. M. (2010) Sucrose octasulfate selectively accelerates thrombin inactivation by heparin cofactor II. *J. Biol. Chem. 285*, 8278−8289.

(28) Carter, W. J., Cama, E., and Huntington, J. A. (2005) Crystal structure of thrombin bound to heparin. *J. Biol. Chem. 280*, 2745−2749.

(29) Kamath, P., Huntington, J. A., and Krishnaswamy, S. (2010) Ligand binding shuttles thrombin along a continuum of zymogen- and proteinase-like states. *J. Biol. Chem. 285*, 28651−28658.

(30) Evans, S. A., Olson, S. T., and Shore, J. D. (1982) p-Aminobenzamidine as a fluorescent probe for the active site of serine proteases. *J. Biol. Chem. 257*, 3014−3017.

(31) Olson, S. T. (1988) Transient kinetics of heparin-catalyzed protease inactivation by antithrombin III. Linkage of protease-inhibitor-heparin interactions in the reaction with thrombin. *J. Biol. Chem. 263*, 1698−1708.

(32) Cochran, S., Li, C. P., and Ferro, V. (2009) A surface plasmon resonance-based solution affinity assay for heparan sulfate-binding proteins. *Glycoconjugate J. 26*, 577−587.

(33) Henry, B. L., Abdel Aziz, M., Zhou, Q., and Desai, U. R. (2010) Sulfated, low molecular weight lignins are potent inhibitors of plasmin, in addition to thrombin and factor Xa: Novel opportunity for controlling complex pathologies. *Thromb. Haemostasis 103*, 507−515.

(34) Iyaguchi, D., Yao, M., Watanbe, N., Tanaka, I., and Toyota, E. (2007) Crystallization and preliminary X-ray studies of the unliganded wild-type bovine thrombin. *Protein Pept. Lett. 14*, 923−924.

(35) García de la Torre, J., Huertas, M. L., and Carrasco, B. (2000) Calculation of hydrodynamic properties of globular proteins from their atomic-level structure. *Biophys. J. 78*, 719−730.

(36) Al-Horani, R. A., and Desai, U. R. (2010) Chemical sulfation of small molecules: Advances and challenges. *Tetrahedron 66*, 2907−2918.

(37) Volkman, B. F., Lipson, D., Wemmer, D. E., and Kern, D. (2001) Two-state allosteric behavior in a single-domain signaling protein. *Science 291*, 2429−2433.

(38) Kern, D., and Zuiderweg, E. R. (2003) The role of dynamics in allosteric regulation. *Curr. Opin. Struct. Biol. 13*, 748−757.

(39) Popovych, N., Sun, S., Ebright, R. H., and Kalodimos, C. G. (2006) Dynamically driven protein allostery. *Nat. Struct. Mol. Biol. 13*, 831−838.